AMERICAN SOCIETY FOR MICROBIOLOGY | Antimicrobial Agents and Chemotherapy®

EXPERIMENTAL THERAPEUTICS

A Human Biofilm-Disrupting Monoclonal Antibody Potentiates Antibiotic Efficacy in Rodent Models of both *Staphylococcus aureus* and *Acinetobacter baumannii* Infections

Yan Q. Xiong,[a,b] Angeles Estellés,[c] L. Li,[a] W. Abdelhady,[a] R. Gonzales,[a] Arnold S. Bayer,[a,b] Edgar Tenorio,[c] Anton Leighton,[c] Stefan Ryser,[c] Lawrence M. Kauvar[c]

Los Angeles Biomedical Research Institute at Harbor-UCLA Medical Center, Torrance, California, USA[a]; David Geffen School of Medicine at UCLA, Los Angeles, California, USA[b]; Trellis Bioscience, LLC, Menlo Park, California, USA[c]

ABSTRACT Many serious bacterial infections are antibiotic refractory due to biofilm formation. A key structural component of biofilm is extracellular DNA, which is stabilized by bacterial proteins, including those from the DNABII family. TRL1068 is a high-affinity human monoclonal antibody against a DNABII epitope conserved across both Gram-positive and Gram-negative bacterial species. In the present study, the efficacy of TRL1068 for the disruption of biofilm was demonstrated *in vitro* in the absence of antibiotics by scanning electron microscopy. The *in vivo* efficacy of this antibody was investigated in a well-characterized catheter-induced aortic valve infective endocarditis model in rats infected with a methicillin-resistant *Staphylococcus aureus* (MRSA) strain with the ability to form thick biofilms, obtained from the blood of a patient with persistent clinical infection. Animals were treated with vancomycin alone or in combination with TRL1068. MRSA burdens in cardiac vegetations and within intracardiac catheters, kidneys, spleen, and liver showed significant reductions in the combination arm versus vancomycin alone ($P < 0.001$). A trend toward mortality reduction was also observed ($P = 0.09$). In parallel, the *in vivo* efficacy of TRL1068 against a multidrug-resistant clinical *Acinetobacter baumannii* isolate was explored by using an established mouse model of skin and soft tissue catheter-related biofilm infection. Catheter segments infected with *A. baumannii* were implanted subcutaneously into mice; animals were treated with imipenem alone or in combination with TRL1068. The combination showed a significant reduction of catheter-adherent bacteria versus the antibiotic alone ($P < 0.001$). TRL1068 shows excellent promise as an adjunct to standard-of-care antibiotics for a broad range of difficult-to-treat bacterial infections.

KEYWORDS *Acinetobacter*, MRSA, biofilms, infective endocarditis, monoclonal antibody, skin and soft tissue infection

Received 28 April 2017 **Returned for modification** 3 June 2017 **Accepted** 11 July 2017

Accepted manuscript posted online 17 July 2017

Citation Xiong YQ, Estellés A, Li L, Abdelhady W, Gonzales R, Bayer AS, Tenorio E, Leighton A, Ryser S, Kauvar LM. 2017. A human biofilm-disrupting monoclonal antibody potentiates antibiotic efficacy in rodent models of both *Staphylococcus aureus* and *Acinetobacter baumannii* infections. Antimicrob Agents Chemother 61:e00904-17. https://doi.org/10.1128/AAC.00904-17.

Address correspondence to Lawrence M. Kauvar, lkauvar@trellisbio.com.

Many serious bacterial infections are difficult to treat due to concomitant biofilm formation, which (i) shields the bacteria from host immunity and (ii) induces a sessile phenotype refractory to antibiotic therapy versus planktonic-state organisms (1). The antibiotic susceptibility of biofilm-associated bacteria is often reduced, as evidenced by the increased MICs for such isolates by as much as 1,000-fold (2). It is estimated that 65 to 80% of clinically significant bacterial infections are biofilm mediated (3), including infective endocarditis (IE) on native and prosthetic valves, osteomyelitis, lung infections associated with cystic fibrosis and chronic obstructive pulmonary

disease (COPD), infections associated with other device implants and catheters, and chronic nonhealing wounds.

A strategy for treating biofilm-associated bacteria that has been intensively explored for more than 2 decades is to interfere with quorum sensing, the chemical communication system used to coordinate the expression of virulence factors. Although compounds that interfere with such signaling molecules have been found (4), no such compound has achieved FDA approval.

There has been increasing interest in disrupting the biofilm structure (5) so as to restore the susceptibility of the biofilm-dispersed bacteria to available antibiotics as well as to reexpose such isolates to immune system control (6). Biofilm is not simply a random assembly of bacterial debris and host components but rather includes specific proteins (7–10) and polymers (11), notably including extracellular DNA (eDNA) (12). The importance of eDNA in the biofilm matrix, which appears to arise primarily from stochastic programmed lysis of bacterial cells (13), has been well established by showing that the DNA-degrading enzyme, DNase, disrupts established biofilms (14, 15). The eDNA forms a three-dimensional mesh-like structure (16) that excludes host immune cells while allowing the diffusion of both nutrients and waste. The eDNA is stabilized by bacterial proteins that bind DNA in a sequence-nonspecific fashion, including type IV pilin (17) and members of the DNABII family (18). The DNABII family comprises integration host factor (IHF) and histone-like DNA-binding (HU) proteins, with conserved homologs in a wide variety of bacterial species (19). The addition of exogenous DNABII protein increases biofilm formation *in vitro*, an effect abolished by DNase (20). Polyclonal sera against a variety of biofilm-associated proteins have been reported to disrupt biofilms (21–24). Human monoclonal antibodies (MAbs) against lipoteichoic acid, an antigen present in the cell wall of most Gram-positive bacteria, have also shown efficacy against drug-resistant *Staphylococcus aureus* in a murine peritonitis model (25). Taken together, data from these studies establish the feasibility, in principle, of an antibody-based intervention to overcome antibiotic resistance in difficult-to-treat biofilm-associated infections.

As we have described previously (26), TRL1068 is a high-affinity MAb directed against the DNABII protein family discovered by screening ~5 million human B lymphocytes using CellSpot technology (27). The conformational epitope on DNABII proteins was determined by high-resolution peptide mapping, including alanine scanning (26). This epitope is in the region implicated in DNA binding (28), which may account for the high degree of conservation. A BLAST search found hundreds of DNABII homologs in which this epitope is highly conserved, across a wide range of bacterial species, including nearly all of the pathogens in the CDC report *Antibiotic Resistance Threats in the United States* (29), allowing the prediction that TRL1068 could have broad antibiofilm efficacy. Efficacy is also expected on the basis of sequence data for the ESKAPE pathogens (*Enterococcus faecium*, *Staphylococcus aureus*, *Klebsiella pneumoniae*, *Acinetobacter baumannii*, *Pseudomonas aeruginosa*, and *Enterobacter* spp.).

The disruption of biofilms *in vitro* by polyclonal sera raised against a DNABII protein has been shown to work by the extraction of the protein from the biofilm (30), for which the high affinity of TRL1068 is a favorable property. TRL1068 activity against biofilms of both *P. aeruginosa* and *S. aureus* was previously demonstrated by scanning electron microscopy (SEM) examination of biofilm-coated surfaces; also, the efficacy *in vivo* of this MAb was demonstrated in a murine implant infection model (26).

In the current investigation, we extend these results to two additional rodent models: a rat model of IE caused by methicillin-resistant *S. aureus* (MRSA) and a murine model of skin and soft tissue infection caused by multidrug-resistant *A. baumannii* (which extends the *in vivo* efficacy data from Gram-positive to Gram-negative bacteria).

RESULTS

Biofilm disruption *in vitro*. (31). Colonized pegs were exposed to TRL1068 or an IgG1 isotype control MAb, each at 0.4 and 1.2 μg/ml, for 12 h, and adherent bacteria were then visualized by SEM. No antibiotics were used in this experiment. As shown in

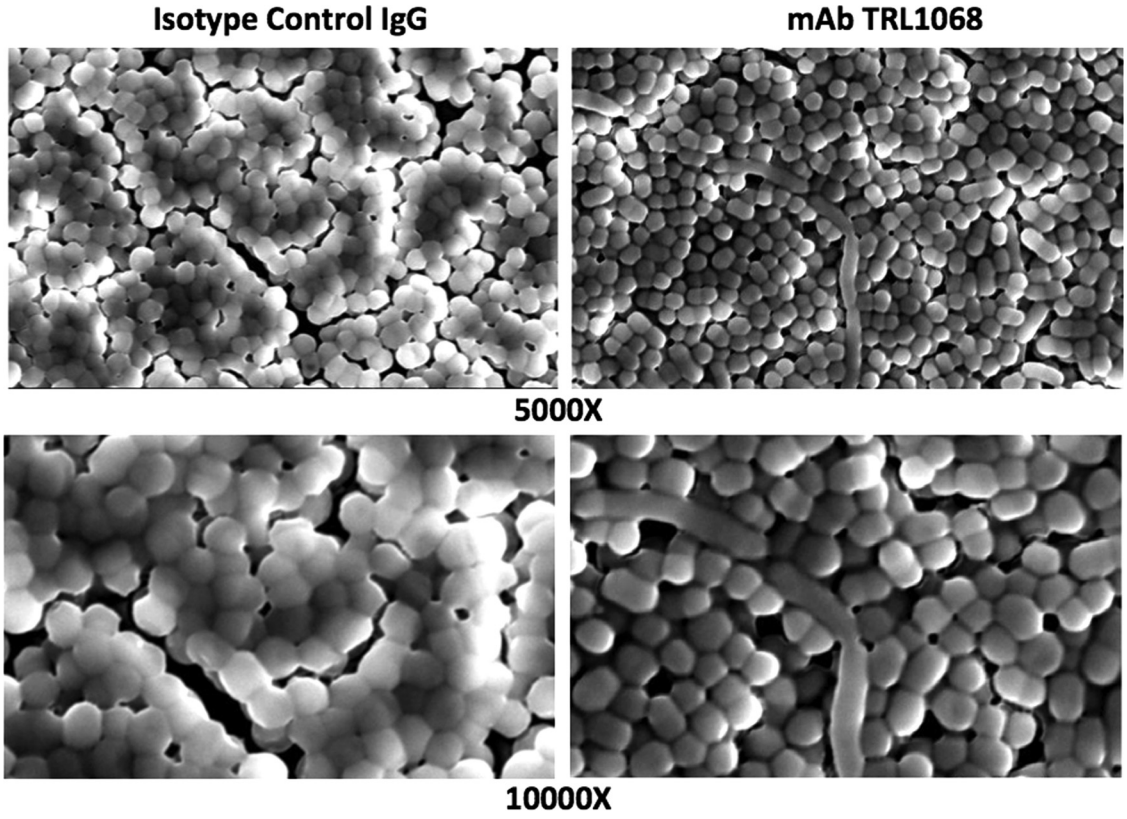

FIG 1 Disruption of biofilms *in vitro*. Bacterial biofilm was formed on conical plastic pegs in a 96-well format. Pegs were treated with IgG isotype control MAb (left) or TRL1068 (right) at 1.2 μg/ml for 12 h. Adherent *A. baumannii* bacterial cells were visualized by SEM at $\times$5,000 and $\times$10,000 magnifications. TRL1068-treated pegs have a thinner biofilm and bacterial cells are less densely packed than on the control pegs.

Fig. 1, the biofilm of *A. baumannii* on the control peg was thicker and the bacteria were more densely packed than those on the TRL1068-treated pegs. These results are consistent with TRL1068-induced biofilm disruption.

Rat IE model. No microbiological differences were seen between the isotype control arm and the vancomycin-alone treatment arm. The vancomycin-plus-TRL1068 treatment arm showed statistically significant reductions in target tissue MRSA bioburdens. For example, compared to the isotype-control-plus-vancomycin arm, there was a median reduction of $\sim$2.0 $\log_{10}$ CFU/g in the cardiac valvular and indwelling catheter vegetations ($P < 0.001$) (Fig. 2A). Kidney, spleen, and liver MRSA bioburdens were also statistically significantly lower in the vancomycin-plus-TRL1068 arm than in the controls (Fig. 2B). This rat IE model had a high mortality rate: 6 of 8 untreated animals died within the study period, as did 6 of 10 of the animals receiving only vancomycin. In contrast, there was a trend toward reduced mortality ($P = 0.09$) for the vancomycin-plus-TRL1068 arm, for which only 3 of 10 animals died (Fig. 2C), compared to animals treated with vancomycin alone.

Murine skin and soft tissue infection model. In study I (Fig. 3A), imipenem alone and imipenem plus the isotype control MAb were minimally effective in reducing *A. baumannii* bioburdens compared to those in the untreated group. Due to imipenem's short half-life in mice ($\sim$15 min) (32) and the frequency of dosing (twice a day [BID]), we estimated that the imipenem plasma concentration dropped below the MIC (2.0 μg/ml for the *A. baumannii* strain used in this experiment) approximately 2 h after the administration of each dose. Nonetheless, in combination with TRL1068, the efficacy of imipenem was significantly improved compared to those in untreated animals and animals treated with imipenem plus the isotype control (-0.8 and -0.5 $\log_{10}$ CFU/catheter, respectively; $P \leq 0.009$).

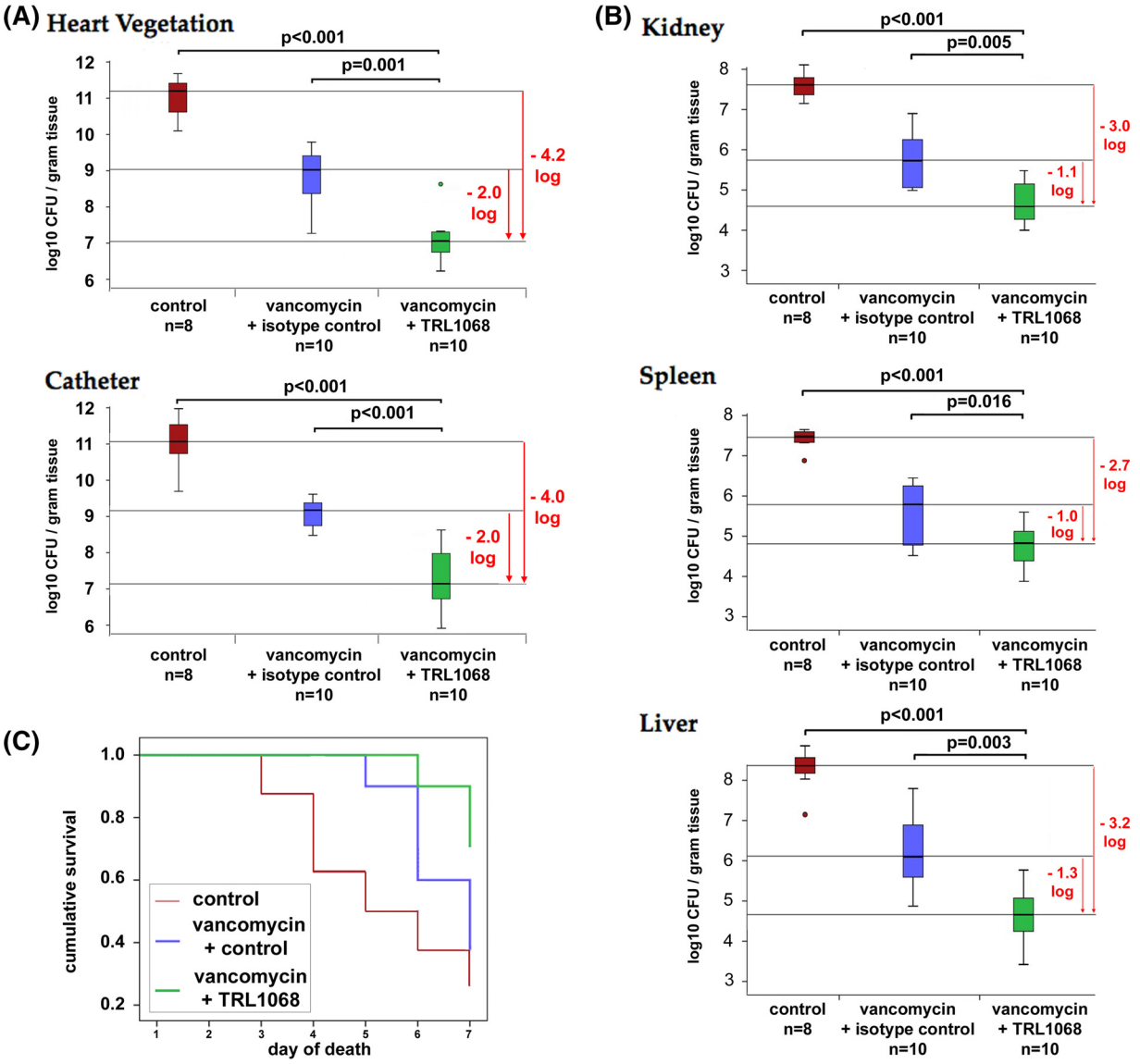

FIG 2 *In vivo* efficacy of TRL1068 with or without vancomycin (VAN) in a rat infective endocarditis model due to MRSA. Median and quartile values are shown, with outliers being denoted by circles. (A) Bacterial burdens of vegetation at the primary site of infection were significantly reduced by 2 logs when TRL1068 was added to vancomycin. (B) An ~1-log reduction of infection was seen at secondary infection sites. (C) Combination therapy resulted in reduced mortality.

In our previous study (26), similar dosing of TRL1068 (15 mg/kg of body weight intraperitoneally [i.p.]) in mice resulted in peak serum levels of >50 mg/liter, with serum levels being maintained well above the effective concentration *in vitro* for over a week (Fig. 1). Accordingly, for study II (Fig. 3B), we kept the TRL1068 dose the same but increased the dose of imipenem from 100 to 150 mg/kg and increased the frequency of dosing from BID to four times a day (QID). One last dose of imipenem was given 4 h before sacrifice. These modifications of the study I protocol were designed to assess the impact of the imipenem dose strategy on outcome in this model. These increased exposures to imipenem alone did not significantly reduce the catheter bioburden compared to that in study I (−0.2 versus −0.3 $\log_{10}$ CFU/catheter). In contrast, increased exposure to imipenem in combination with TRL1068 showed a significant improvement in efficacy compared to untreated mice and mice treated with imipenem plus the isotype control MAb (−1.8 and −1.6 $\log_{10}$ CFU/catheter, respectively; $P <$ 0.001). The bacteria extracted from the catheters at the end of the experiment showed

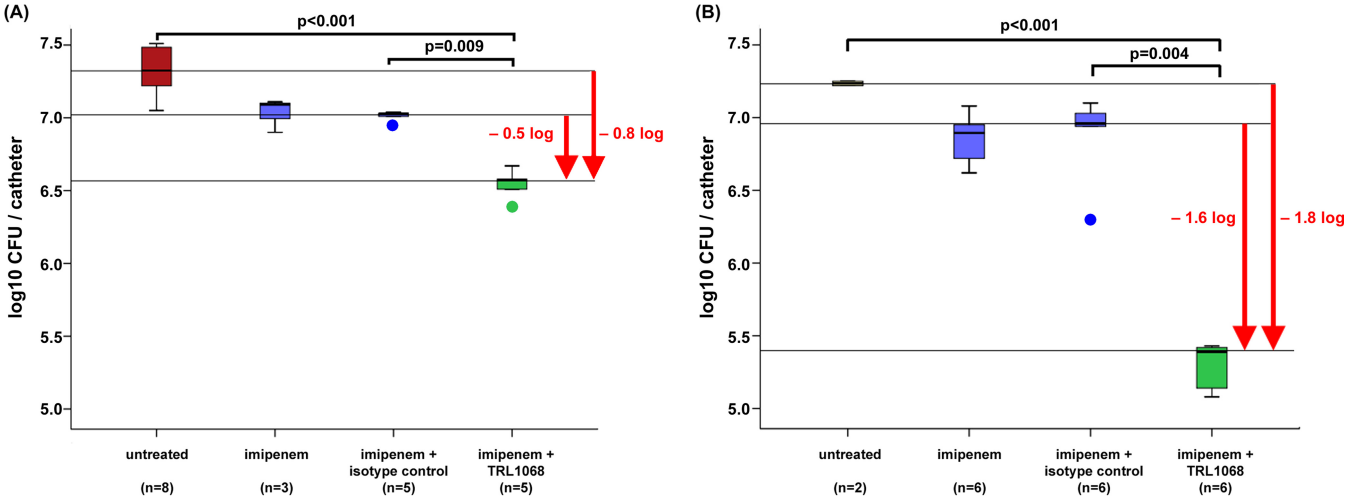

FIG 3 *In vivo* efficacy of TRL1068 with or without imipenem (IPM) in a murine catheter-related skin and soft tissue infection model due to a multidrug-resistant *A. baumannii* strain. Median and quartile values are shown, with outliers being denoted by circles. TRL1068 potentiates imipenem activity against *A. baumannii* (10^6 CFU). (A) Imipenem at 100 mg/kg BID; (B) imipenem at 150 mg/kg QID. For data in both panels, TRL1068 was given at 15 mg/kg on days 1 and 4; the control includes an isotype control nonimmune MAb.

no growth on plates containing imipenem at 8 mg/liter, indicating that there was no development of imipenem resistance during the 6 days of treatment.

DISCUSSION

Leveraging the immune system to combat infectious diseases has a long and successful history (33). Although the primary focus has been on vaccines over the past 50 years, in the early 20th century, serum therapy was used effectively against many infectious diseases (34). Due to serum sickness and immediate hypersensitivity issues, this treatment mode was largely abandoned during the antibiotic era. Given the relatively limited discovery of new antibiotics in recent decades and the development of well-tolerated monoclonal antibodies, there has been a resurgence of interest in such treatments, especially for bacterial infections (34).

Bacterial biofilm is a major contributor to antibiotic treatment failures in a variety of clinical settings (1, 3), particularly as the unmet medical need has shifted from acute community-acquired infections to more chronic infections associated with health care contact (35). The prevention or disruption of biofilms thus represents an important albeit elusive clinical goal. Antibody-based antibiofilm therapy has shown promise in preclinical models targeting several different biofilm components (21–25), including the DNABII protein family (18, 26, 36), for which synergy with antibiotics has been shown for a polyclonal antibody (18).

TRL1068 is a native human MAb that binds with high affinity to a broad spectrum of DNABII proteins from both Gram-positive and Gram-negative bacteria (26). At a concentration of 1.2 μg/ml *in vitro*, it disrupts established biofilm over the course of 12 h in *S. aureus*, *P. aeruginosa* (26), and *A. baumannii* (shown here). Previous pharmacokinetic studies with TRL1068 in mice demonstrated that a dose of 15 mg/kg results in peak serum levels of $>$50 μg/ml, with serum levels being maintained well above the effective concentration *in vitro* for over a week (26).

TRL1068 has now shown robust efficacy in potentiating conventional antibiotics in three distinct animal models of infection involving biofilm formation.

First, in a murine tissue cage soft tissue *S. aureus* infection model (37, 38), daptomycin combined with TRL1068 significantly reduced the levels of both planktonic bacteria and adherent bacteria and completely eradicated infection when used prophylactically (26).

Second, as detailed in the present investigation using a model of MRSA IE in rats (39, 40), vancomycin alone yielded an $\sim$2.0-$\log_{10}$ CFU/g reduction in the MRSA bioburden

in cardiac vegetations, whereas vancomycin in combination with TRL1068 resulted in an ~4.0-$\log_{10}$ CFU/g reduction in MRSA bioburdens in cardiac vegetations relative to those in untreated controls. Similar enhanced reductions in bioburdens in several other target organs (kidneys, spleen, and liver) were demonstrated. Given the slow bactericidal effect of vancomycin against *S. aureus* (41), the substantial synergy of TRL1068 with vancomycin in this study strongly suggests future clinical translatability in MRSA bacteremia and IE.

Third, as also detailed in the present investigation, a model that was originally developed to mimic tunneled catheter infections in patients receiving hemodialysis was used (42). However, this model is equally relevant to other soft tissue infections, including chronic nonhealing wounds, for which biofilm is often implicated in the persistence of infection (43). By using a hospital-derived antibiotic-resistant strain of *A. baumannii* (42), an increasingly important Gram-negative pathogen, TRL1068 in combination with imipenem showed enhanced reductions in bacterial bioburdens compared to those in animals treated with imipenem alone and with imipenem plus an isotype control MAb as well as in untreated control animals. Of interest, this salutary impact was achieved despite the fact that TRL1068 is continuously degrading the biofilm, allowing the released bacteria to revert to the faster-growing planktonic state during the intervals in which the imipenem concentration drops below the MIC for the *A. baumannii* isolate. The dose and the frequency of imipenem administration had a strong effect on the efficacy of a fixed dose of TRL1068 plus imipenem, with efficacy increasing as the imipenem dosage and frequency of administration were each increased. These results are consistent with the proposed mechanism for such "synergy," namely, that the biofilm-disrupting property of the MAb potentiates antibiotic activity via enhanced access to the organism and reversion to the more-drug-sensitive planktonic state rather than the MAb having a direct bactericidal activity of its own. The best data on time-kill activity for imipenem are for *P. aeruginosa* (44), for which concentration dependence has been shown over a range of 0.25 to 4 times the MIC, requiring ~5 h to reach 99.9% kill. Maximal bactericidal effect is achieved when the free-drug concentration exceeds the targeted pathogen's MIC by approximately 4-fold for 40 to 60% of the dosing interval (45). Since the half-life of imipenem in humans is longer than that in mice, and more frequent dosing strategies are more feasible in the clinical setting (46, 47), the efficacy of TRL1068 in combination with such antibiotics for clinical soft tissue infections may well exceed that observed in this murine model.

The highly conserved TRL1068-binding epitope on DNABII proteins across extensive phylogenetic distances (26) suggests that its use as adjunct therapy in combination with standard-of-care antibiotics will provide a significant improvement in the treatment of a broad spectrum of biofilm-associated infections, including polymicrobial infections. This broad-spectrum effect is a favorable feature compared to recently described murine hybridoma MAbs against DNABII proteins, for which a mixture of two MAbs was more effective than either MAb alone (36).

Clinically significant resistance to TRL1068 is expected to be rare for several reasons. First, mutations in the epitope region are known to affect DNA binding (28), suggesting that TRL1068 escape mutations will decrease the functionality of this required site on the protein. An analogous reduced fitness for MAb escape mutants has been reported for similarly conserved epitopes on several viruses (48, 49). Second, DNABII proteins are dimers, with some bacterial species expressing alpha and beta subunits of both HU and IHF. In the case of *P. aeruginosa*, TRL1068 binds to both IHF subunits but only one of the heterodimeric HU subunits, yet it is still able to disrupt the biofilm. This implies that escape from TRL1068 will require concurrent mutations in more than one subunit, further reducing the likelihood of the development of resistance against this new treatment modality. Third, the release of the DNABII protein into the extracellular matrix occurs primarily via the stochastic lysis of a subset of the bacterial pathogens in the biofilm (13). A TRL1068 escape mutant will have no additional survival value, as it will already be dead when its proteins are confronted by TRL1068. Thus, there will be no selective pressure for escape mutations.

The *in vivo* studies described here strongly support the development of human MAb TRL1068 for the treatment of biofilm-associated infections in combination with standard-of-care antibiotics.

MATERIALS AND METHODS

Monoclonal antibodies. TRL1068 (10 mg/ml) and an IgG1 isotype control MAb (7.4 mg/ml) in phosphate-buffered saline (PBS) (pH 7.4) were provided by Trellis Bioscience, LLC (Menlo Park, CA).

Antibiotics. Vancomycin was purchased from American Pharmaceutical Partners Inc. (Los Angeles, CA). The antibiotic was reconstituted in appropriate diluents, as recommended by the manufacturers. Imipenem was injected along with cilastatin (marketed as Primaxin in the United States); cilastatin, a specific inhibitor of renal dehydropeptidase-1 (DHP-1), increases the systemic half-life of imipenem, a broad-spectrum beta-lactam.

Bacteria. The biofilm-forming MRSA strain (HA-MRSA 300-169) is a hospital-acquired clinical isolate from a patient with persistent bacteremia (≥14 days of positive MRSA blood cultures) despite receiving antibiotics to which the isolate was susceptible *in vitro*; importantly, this MRSA strain can form thick biofilms (50, 51). Its MIC of vancomycin is 0.5 μg/ml. The multidrug-resistant *A. baumannii* strain employed in this investigation was isolated at Harbor-UCLA Medical Center (HUMC-12) from a diabetic stump wound infection (52). It is susceptible to a limited number of antibiotics, including imipenem (used in this study), with an MIC of 2.0 μg/ml.

***In vitro* biofilm-disrupting assay.** As previously described (26), the biofilm-disrupting activity of TRL1068 was evaluated by using the minimum biofilm eradication concentration (MBEC) assay performed by Innovotech Inc. (Edmonton, Alberta, Canada). The MBEC device consists of conical plastic pegs in a 96-well-microplate format, with multiple parameters optimized to grow a reproducible biofilm (31). According to procedures used previously for *S. aureus* and *P. aeruginosa* (26), a subclone from a cryogenic stock derived from a clinical isolate of *A. baumannii* was generated by streaking cultures onto tryptic soy agar plates, and aliquots were transferred into the wells of the MBEC device, which was incubated at 37°C on an orbital shaker (110 rpm) for 24 h for biofilm growth. The peg array was transferred to a sterile 96-well microtiter rinse plate (200 μl per well of 0.9% sterile saline) for 1 to 2 min and then transferred to a challenge plate and treated with the vehicle, IgG1 isotype control MAb, or TRL1068 at 0.4 and 1.2 μg/ml for 12 h. Adherent bacteria were fixed by using 5% glutaraldehyde in 0.1 M sodium cacodylate buffer (pH 7.5) (at 4°C for 24 h and then air dried). The pegs were attached to aluminum stubs and sputter coated with a conductive layer (Platinum-Gold). The attached bacteria were visualized by SEM (catalog number S3700N; Hitachi) at magnifications ranging from ×30 to ×10,000.

Rat infective endocarditis model. (i) Model. Female Sprague-Dawley rats (250 to 300 g each) were obtained from Harlan Inc. (Indianapolis, IN). All animals were housed in our animal facility on-site. All experimental procedures were approved by our intramural Institutional Animal Care and Use Committee. A well-established experimental rat IE model was used in the present studies (39, 53). Animals were anesthetized with an isoflurane-oxygen gas mixture (2% isoflurane) during surgery. An indwelling polyethylene catheter was positioned in the left ventricle of each animal via the retrograde transcarotid artery approach, with the tip passing across the aortic valve, thereby inducing sterile vegetations. The catheter was left in place throughout the study. At 3 days postcatheterization, animals were infected intravenously (i.v.) through the tail vein with an inoculum of $\sim 10^5$ CFU of HA-MRSA 300-169 to induce IE. This inoculum represents the 95% infective dose (ID_{95}) for this strain in the rat IE model. Animals that either became moribund or were in poor medical condition were euthanized, target tissues were collected when possible, and the day of death was recorded. All surviving animals were euthanized on day 7 with 200 mg/kg sodium pentobarbital given as a rapid bolus intraperitoneally.

(ii) Treatment. At 24 h postinfection, animals were randomized to receive (i) saline (untreated control; every 12 h [q12h] subcutaneously), (ii) vancomycin (120 mg/kg q12h subcutaneously for 6 days) (54), (iii) vancomycin (120 mg/kg q12h subcutaneously for 6 days) plus an isotype control MAb (15 mg/kg i.v. on days 1 and 4 before administration of vancomycin), or (iv) vancomycin (120 mg/kg q12h subcutaneously for 6 days) plus TRL1068 (15 mg/kg i.v. on days 1 and 4 before administration of vancomycin). The number of animals ranged from 8 to 10 per group.

(iii) Sacrifices. Twenty-four hours after the last vancomycin treatment, animals were sacrificed, and all cardiac and catheter vegetations and liver, kidney, and spleen samples were obtained, weighed, homogenized in saline, serially diluted, and plated onto tryptic soy agar (TSA) plates for quantitative culture (data were expressed as median CFU per gram and quartiles). All cultures were grown for 24 h at 37°C prior to counting.

Murine skin and soft tissue infection model. (i) Model. BALB/c mice (female, 18 to 22 g) were obtained from Harlan Inc. (Indianapolis, IN). All animals were housed in the animal facility on-site, and all experimental procedures adhered to a protocol approved by the Institutional Animal Care and Use Committee. Infection was induced by implanting a precolonized Teflon catheter segment (1 cm) inoculated with 10^6 CFU/catheter of *A. baumannii* strain HUMC-12. Animals were anesthetized by using an isoflurane-oxygen gas mixture (2% isoflurane) during catheter implantation (42). Their flanks were shaved, and the skin was cleansed with povidone-iodine (Betadyne) and alcohol. A 2- to 3-mm skin incision was made and dissected to create a subcutaneous tunnel, into which a 1-cm segment of each infected catheter was implanted at a distance of at least 1 cm from the incision. The incision was then covered with intact skin and closed with sterile surgical staples. One catheter segment was inserted on each side of each animal (42).

Based on our extensive studies using this model (42), the catheter segment infected with an ID_{95} induces substantial subcutaneous catheter-associated soft tissue infection. Two parallel treatment studies were performed to allow evaluation of the effects of more intensive antibiotic treatment on outcome, taking into account the short half-life of imipenem in mice.

(ii) Study I. Twenty-four hours after the catheter was implanted, animals were randomized into the following groups: (i) controls without any treatment, (ii) imipenem alone (100 mg/kg i.p. BID for 6 days) (55, 56), (iii) imipenem (100 mg/kg i.p. BID for 6 days) and an IgG isotype control MAb (15 mg/kg i.p. on days 1 and 4 before administration of imipenem), or (iv) imipenem (100 mg/kg i.p. BID for 6 days) and TRL1068 (15 mg/kg i.p. on days 1 and 4 before administration of imipenem). All animals were euthanized on day 7.

(iii) Study II. Twenty-four hours after the catheter was implanted, animals were randomized into the following groups: (i) controls without any treatment, (ii) imipenem (150 mg/kg i.p. QID for 6 days) (57), (iii) imipenem (150 mg/kg i.p. QID for 6 days) plus an IgG isotype control MAb (15 mg/kg i.p. on days 1 and 4 before administration of imipenem), or (iv) imipenem (150 mg/kg i.p. QID for 6 days) plus TRL1068 (15 mg/kg i.p. on days 1 and 4 before administration imipenem). In addition, on the seventh day, animals in the second, third, and fourth groups were given an additional dose of imipenem. All animals were sacrificed ~4 h after the last imipenem dose. The plasma half-life of imipenem is <15 min in mouse (32). Imipenem plasma concentrations were likely below the MIC by the time when the animals were sacrificed, and it takes several hours for full reversion to the planktonic state (41). The antibiotic carryover effect for bacterial quantitation *in vitro* was therefore negligible.

(iv) Sacrifices. At sacrifice, catheters were removed and placed into a separate tube containing 1 ml of PBS. The tubes were sonicated for 30 s three times and then vortexed for 1 min to remove all catheter- and biofilm-associated bacteria from the support surface. Solutions were serially diluted and plated onto TSA plates for quantitative culture (group data calculated as median CFU per catheter and quartiles). All cultures were grown for 24 h at 37°C. For study II, at sacrifice, catheters were removed for quantitative culture on TSA plates with or without imipenem at 8 mg/liter (*A. baumannii* resistance breakpoint) (58).

Statistical analysis. MRSA and *A. baumannii* bacterial burdens (log_{10} CFU per gram or per catheter) in target tissues and on catheter segments, respectively, were compared between treatment groups by using nonparametric testing. The Kruskal-Wallis test was used to determine whether the median log_{10} CFU per gram or per catheter between groups were different. Box plots were used to present the data. Statistical analysis and plotting were performed by using IBM SPSS Statistics version 20 (IBM, Armonk, NY). A P value of <0.05 was considered significant.

ACKNOWLEDGMENTS

All of the studies reported here were funded by Trellis Bioscience, LLC, including partial funding from an SBIR grant from the U.S. National Institute of Allergy and Infectious Disease (R44 AI120425). The *in vivo* experiments at the Los Angeles Biomedical Research Institute at Harbor-UCLA Medical Center were funded through a contract with Trellis Bioscience, LLC; those investigators have no other financial interest in Trellis. All other authors are paid employees or consultants of Trellis Bioscience.

REFERENCES

1. Lebeaux D, Chauhan A, Rendueles O, Beloin C. 2013. From in vitro to in vivo models of bacterial biofilm-related infections. Pathogens 2:288–356. https://doi.org/10.3390/pathogens2020288.
2. Wu H, Moser C, Wang HZ, Hoiby N, Song ZJ. 2015. Strategies for combating bacterial biofilm infections. Int J Oral Sci 7:1–7. https://doi.org/10.1038/ijos.2014.65.
3. Coenye T, Nelis HJ. 2010. In vitro and in vivo model systems to study microbial biofilm formation. J Microbiol Methods 83:89–105. https://doi.org/10.1016/j.mimet.2010.08.018.
4. Rabin N, Zheng Y, Opoku-Temeng C, Du Y, Bonsu E, Sintim HO. 2015. Agents that inhibit bacterial biofilm formation. Future Med Chem 7:647–671. https://doi.org/10.4155/fmc.15.7.
5. Chew SC, Kundukad B, Seviour T, van der Maarel JR, Yang L, Rice SA, Doyle P, Kjelleberg S. 2014. Dynamic remodeling of microbial biofilms by functionally distinct exopolysaccharides. mBio 5:e0153-14. https://doi.org/10.1128/mBio.01536-14.
6. Boles BR, Horswill AR. 2011. Staphylococcal biofilm disassembly. Trends Microbiol 19:449–455. https://doi.org/10.1016/j.tim.2011.06.004.
7. Brady RA, Leid JG, Camper AK, Costerton JW, Shirtliff ME. 2006. Identification of Staphylococcus aureus proteins recognized by the antibody-mediated immune response to a biofilm infection. Infect Immun 74:3415–3426. https://doi.org/10.1128/IAI.00392-06.
8. Huseby MJ, Kruse AC, Digre J, Kohler PL, Vocke JA, Mann EE, Bayles KW, Bohach GA, Schlievert PM, Ohlendorf DH, Earhart CA. 2010. Beta toxin catalyzes formation of nucleoprotein matrix in staphylococcal biofilms. Proc Natl Acad Sci U S A 107:14407–14412. https://doi.org/10.1073/pnas.0911032107.
9. Jiao Y, D'Haeseleer P, Dill BD, Shah M, Verberkmoes NC, Hettich RL, Banfield JF, Thelen MP. 2011. Identification of biofilm matrix-associated proteins from an acid mine drainage microbial community. Appl Environ Microbiol 77:5230–5237. https://doi.org/10.1128/AEM.03005-10.
10. Kuboniwa M, Hendrickson EL, Xia Q, Wang T, Xie H, Hackett M, Lamont RJ. 2009. Proteomics of Porphyromonas gingivalis within a model oral microbial community. BMC Microbiol 9:98. https://doi.org/10.1186/1471-2180-9-98.
11. Flemming H-C. 2016. EPS—then and now. Microorganisms 4:41. https://doi.org/10.3390/microorganisms4040041.
12. Mann EE, Rice KC, Boles BR, Endres JL, Ranjit D, Chandramohan L, Tsang LH, Smeltzer MS, Horswill AR, Bayles KW. 2009. Modulation of eDNA release and degradation affects Staphylococcus aureus biofilm maturation. PLoS One 4:e5822. https://doi.org/10.1371/journal.pone.0005822.
13. Turnbull L, Toyofuku M, Hynen AL, Kurosawa M, Pessi G, Petty NK, Osvath SR, Carcamo-Oyarce G, Gloag ES, Shimoni R, Omasits U, Ito S, Yap X, Monahan LG, Cavaliere R, Ahrens CH, Charles IG, Nomura N, Eberl L, Whitchurch CB. 2016. Explosive cell lysis as a mechanism for the biogenesis of bacterial membrane vesicles and biofilms. Nat Commun 7:11220. https://doi.org/10.1038/ncomms11220.
14. Shields RC, Mokhtar N, Ford M, Hall MJ, Burgess JG, ElBadawey MR, Jakubovics NS. 2013. Efficacy of a marine bacterial nuclease against

biofilm forming microorganisms isolated from chronic rhinosinusitis. PLoS One 8:e55339. https://doi.org/10.1371/journal.pone.0055339.
15. Whitchurch CB, Tolker-Nielsen T, Ragas PC, Mattick JS. 2002. Extracellular DNA required for bacterial biofilm formation. Science 295:1487. https://doi.org/10.1126/science.295.5559.1487.
16. Jurcisek JA, Bakaletz LO. 2007. Biofilms formed by nontypeable Haemophilus influenzae in vivo contain both double-stranded DNA and type IV pilin protein. J Bacteriol 189:3868–3875. https://doi.org/10.1128/JB.01935-06.
17. Novotny LA, Adams LD, Kang DR, Wiet GJ, Cai X, Sethi S, Murphy TF, Bakaletz LO. 2009. Epitope mapping immunodominant regions of the PilA protein of nontypeable Haemophilus influenzae (NTHI) to facilitate the design of two novel chimeric vaccine candidates. Vaccine 28:279–289. https://doi.org/10.1016/j.vaccine.2009.08.017.
18. Goodman SD, Obergfell KP, Jurcisek JA, Novotny LA, Downey JS, Ayala EA, Tjokro N, Li B, Justice SS, Bakaletz LO. 2011. Biofilms can be dispersed by focusing the immune system on a common family of bacterial nucleoid-associated proteins. Mucosal Immunol 4:625–637. https://doi.org/10.1038/mi.2011.27.
19. Swinger KK, Rice PA. 2004. IHF and HU: flexible architects of bent DNA. Curr Opin Struct Biol 14:28–35. https://doi.org/10.1016/j.sbi.2003.12.003.
20. Devaraj A, Justice SS, Bakaletz LO, Goodman SD. 2015. DNABII proteins play a central role in UPEC biofilm structure. Mol Microbiol 96:1119–1135. https://doi.org/10.1111/mmi.12994.
21. Freire MO, Devaraj A, Young A, Navarro JB, Downey JS, Chen C, Bakaletz LO, Zadeh HH, Goodman SD. 2017. A bacterial-biofilm-induced oral osteolytic infection can be successfully treated by immuno-targeting an extracellular nucleoid-associated protein. Mol Oral Microbiol 32:74–88. https://doi.org/10.1111/omi.12155.
22. Novotny LA, Jurcisek JA, Ward MO, Jr, Jordan ZB, Goodman SD, Bakaletz LO. 2015. Antibodies against the majority subunit of type IV pili disperse nontypeable Haemophilus influenzae biofilms in a LuxS-dependent manner and confer therapeutic resolution of experimental otitis media. Mol Microbiol 96:276–292. https://doi.org/10.1111/mmi.12934.
23. Shahrooei M, Hira V, Stijlemans B, Merckx R, Hermans PW, Van Eldere J. 2009. Inhibition of Staphylococcus epidermidis biofilm formation by rabbit polyclonal antibodies against the SesC protein. Infect Immun 77:3670–3678. https://doi.org/10.1128/IAI.01464-08.
24. Sun D, Accavitti MA, Bryers JD. 2005. Inhibition of biofilm formation by monoclonal antibodies against Staphylococcus epidermidis RP62A accumulation-associated protein. Clin Diagn Lab Immunol 12:93–100.
25. Rossmann FS, Laverde D, Kropec A, Romero-Saavedra F, Meyer-Buehn M, Huebner J. 2015. Isolation of highly active monoclonal antibodies against multiresistant gram-positive bacteria. PLoS One 10:e0118405. https://doi.org/10.1371/journal.pone.0118405.
26. Estelles A, Woischnig AK, Liu K, Stephenson R, Lomongsod E, Nguyen D, Zhang J, Heidecker M, Yang Y, Simon RJ, Tenorio E, Ellsworth S, Leighton A, Ryser S, Gremmelmaier NK, Kauvar LM. 2016. A high-affinity native human antibody disrupts biofilm from Staphylococcus aureus bacteria and potentiates antibiotic efficacy in a mouse implant infection model. Antimicrob Agents Chemother 60:2292–2301. https://doi.org/10.1128/AAC.02588-15.
27. Harriman WD, Collarini EJ, Sperinde GV, Strandh M, Fatholahi MM, Dutta A, Lee Y, Mettler SE, Keyt BA, Ellsworth SL, Kauvar LM. 2009. Antibody discovery via multiplexed single cell characterization. J Immunol Methods 341:135–145. https://doi.org/10.1016/j.jim.2008.11.009.
28. Chen C, Ghosh S, Grove A. 2004. Substrate specificity of Helicobacter pylori histone-like HU protein is determined by insufficient stabilization of DNA flexure points. Biochem J 383:343–351. https://doi.org/10.1042/BJ20040938.
29. Centers for Disease Control and Prevention. 2013. Antibiotic resistance threats in the United States. Centers for Disease Control and Prevention, Atlanta, GA.
30. Brockson ME, Novotny LA, Mokrzan EM, Malhotra S, Jurcisek JA, Akbar R, Devaraj A, Goodman SD, Bakaletz LO. 2014. Evaluation of the kinetics and mechanism of action of anti-integration host factor-mediated disruption of bacterial biofilms. Mol Microbiol 93:1246–1258. https://doi.org/10.1111/mmi.12735.
31. Harrison JJ, Stremick CA, Turner RJ, Allan ND, Olson ME, Ceri H. 2010. Microtiter susceptibility testing of microbes growing on peg lids: a miniaturized biofilm model for high-throughput screening. Nat Protoc 5:1236–1254. https://doi.org/10.1038/nprot.2010.71.
32. Renneberg J, Walder M. 1989. Postantibiotic effects of imipenem, norfloxacin, and amikacin in vitro and in vivo. Antimicrob Agents Chemother 33:1714–1720. https://doi.org/10.1128/AAC.33.10.1714.
33. Graham BS, Ambrosino DM. 2015. History of passive antibody administration for prevention and treatment of infectious diseases. Curr Opin HIV AIDS 10:129–134. https://doi.org/10.1097/COH.0000000000000154.
34. Saylor C, Dadachova E, Casadevall A. 2009. Monoclonal antibody-based therapies for microbial diseases. Vaccine 27(Suppl 6):G38–G46. https://doi.org/10.1016/j.vaccine.2009.09.105.
35. Bjarnsholt T. 2013. The role of bacterial biofilms in chronic infections. APMIS Suppl 121:1–58. https://doi.org/10.1111/apm.12099.
36. Novotny LA, Jurcisek JA, Goodman SD, Bakaletz LO. 16 June 2016. Monoclonal antibodies against DNA-binding tips of DNABII proteins disrupt biofilms in vitro and induce bacterial clearance in vivo. EBioMedicine https://doi.org/10.1016/j.ebiom.2016.06.022.
37. John AK, Schmaler M, Khanna N, Landmann R. 2011. Reversible daptomycin tolerance of adherent staphylococci in an implant infection model. Antimicrob Agents Chemother 55:3510–3516. https://doi.org/10.1128/AAC.00172-11.
38. Nowakowska J, Landmann R, Khanna N. 2014. Foreign body infection models to study host-pathogen response and antimicrobial tolerance of bacterial biofilm. Antibiotics (Basel) 3:378–397. https://doi.org/10.3390/antibiotics3030378.
39. Abdelhady W, Bayer AS, Seidl K, Moormeier DE, Bayles KW, Cheung A, Yeaman MR, Xiong YQ. 2014. Impact of vancomycin on sarA-mediated biofilm formation: role in persistent endovascular infections due to methicillin-resistant Staphylococcus aureus. J Infect Dis 209:1231–1240. https://doi.org/10.1093/infdis/jiu007.
40. Perlman BB, Freedman LR. 1971. Experimental endocarditis. II. Staphylococcal infection of the aortic valve following placement of a polyethylene catheter in the left side of the heart. Yale J Biol Med 44:206–213.
41. Deresinski S. 2007. Counterpoint: vancomycin and Staphylococcus aureus—an antibiotic enters obsolescence. Clin Infect Dis 44:1543–1548. https://doi.org/10.1086/518452.
42. Bayer AS, Abdelhady W, Li L, Gonzales R, Xiong YQ. 2016. Comparative efficacies of tedizolid phosphate, linezolid, and vancomycin in a murine model of subcutaneous catheter-related biofilm infection due to methicillin-susceptible and -resistant Staphylococcus aureus. Antimicrob Agents Chemother 60:5092–5096. https://doi.org/10.1128/AAC.00880-16.
43. Gabrilska RA, Rumbaugh KP. 2015. Biofilm models of polymicrobial infection. Future Microbiol 10:1997–2015. https://doi.org/10.2217/fmb.15.109.
44. Hengzhuang W, Wu H, Ciofu O, Song Z, Hoiby N. 2012. In vivo pharmacokinetics/pharmacodynamics of colistin and imipenem in Pseudomonas aeruginosa biofilm infection. Antimicrob Agents Chemother 56:2683–2690. https://doi.org/10.1128/AAC.06486-11.
45. Craig WA. 1998. Pharmacokinetic/pharmacodynamic parameters: rationale for antibacterial dosing of mice and men. Clin Infect Dis 26:1–10, quiz 11–12. https://doi.org/10.1086/516284.
46. Lodise TP, Lomaestro BM, Drusano GL. 2006. Application of antimicrobial pharmacodynamic concepts into clinical practice: focus on beta-lactam antibiotics. Insights from the Society of Infectious Diseases Pharmacists. Pharmacotherapy 26:1320–1332. https://doi.org/10.1592/phco.26.9.1320.
47. Sakka SG, Glauner AK, Bulitta JB, Kinzig-Schippers M, Pfister W, Drusano GL, Sorgel F. 2007. Population pharmacokinetics and pharmacodynamics of continuous versus short-term infusion of imipenem-cilastatin in critically ill patients in a randomized, controlled trial. Antimicrob Agents Chemother 51:3304–3310. https://doi.org/10.1128/AAC.01318-06.
48. Chai N, Swem LR, Reichelt M, Chen-Harris H, Luis E, Park S, Fouts A, Lupardus P, Wu TD, Li O, McBride J, Lawrence M, Xu M, Tan MW. 2016. Two escape mechanisms of influenza A virus to a broadly neutralizing stalk-binding antibody. PLoS Pathog 12:e1005702. https://doi.org/10.1371/journal.ppat.1005702.
49. Rodrigo C, Walker MR, Leung P, Eltahla AA, Grebely J, Dore GJ, Applegate T, Page K, Dwivedi S, Bruneau J, Morris MD, Cox AL, Osburn W, Kim AY, Schinkel J, Shoukry NH, Lauer GM, Maher L, Hellard M, Prins M, Luciani F, Lloyd AR, Bull RA. 2017. Limited naturally occurring escape in broadly neutralizing antibody epitopes in hepatitis C glycoprotein E2 and constrained sequence usage in acute infection. Infect Genet Evol 49:88–96. https://doi.org/10.1016/j.meegid.2017.01.006.
50. Seidl K, Chen L, Bayer AS, Hady WA, Kreiswirth BN, Xiong YQ. 2011. Relationship of agr expression and function with virulence and vancomycin treatment outcomes in experimental endocarditis due to methicillin-resistant Staphylococcus aureus. Antimicrob Agents Chemother 55:5631–5639. https://doi.org/10.1128/AAC.05251-11.
51. Abdelhady W, Bayer AS, Seidl K, Nast CC, Kiedrowski MR, Horswill AR, Yeaman MR, Xiong YQ. 2013. Reduced vancomycin susceptibility in an in vitro catheter-related biofilm model correlates with poor therapeutic

outcomes in experimental endocarditis due to methicillin-resistant Staphylococcus aureus. Antimicrob Agents Chemother 57:1447–1454. https://doi.org/10.1128/AAC.02073-12.
52. Luo G, Spellberg B, Gebremariam T, Bolaris M, Lee H, Fu Y, French SW, Ibrahim AS. 2012. Diabetic murine models for Acinetobacter baumannii infection. J Antimicrob Chemother 67:1439–1445. https://doi.org/10.1093/jac/dks050.
53. Peerschke EI, Bayer AS, Ghebrehiwet B, Xiong YQ. 2006. gC1qR/p33 blockade reduces Staphylococcus aureus colonization of target tissues in an animal model of infective endocarditis. Infect Immun 74:4418–4423. https://doi.org/10.1128/IAI.01794-05.
54. Xiong YQ, Willard J, Kadurugamuwa JL, Yu J, Francis KP, Bayer AS. 2005. Real-time in vivo bioluminescent imaging for evaluating the efficacy of antibiotics in a rat Staphylococcus aureus endocarditis model. Antimicrob Agents Chemother 49:380–387. https://doi.org/10.1128/AAC.49.1.380-387.2005.
55. Gudmundsson S, Vogelman B, Craig WA. 1986. The in-vivo postantibiotic effect of imipenem and other new antimicrobials. J Antimicrob Chemother 18(Suppl E):67–73. https://doi.org/10.1093/jac/18.Supplement_E.67.
56. Lepeule R, Ruppe E, Le P, Massias L, Chau F, Nucci A, Lefort A, Fantin B. 2012. Cefoxitin as an alternative to carbapenems in a murine model of urinary tract infection due to Escherichia coli harboring CTX-M-15-type extended-spectrum beta-lactamase. Antimicrob Agents Chemother 56:1376–1381. https://doi.org/10.1128/AAC.06233-11.
57. Soubirou JF, Rossi B, Couffignal C, Ruppe E, Chau F, Massias L, Lepeule R, Mentre F, Fantin B. 2015. Activity of temocillin in a murine model of urinary tract infection due to Escherichia coli producing or not producing the ESBL CTX-M-15. J Antimicrob Chemother 70:1466–1472. https://doi.org/10.1093/jac/dku542.
58. Lee YT, Chiang MC, Kuo SC, Wang YC, Lee IH, Chen TL, Yang YS. 2016. Carbapenem breakpoints for Acinetobacter baumannii group: supporting clinical outcome data from patients with bacteremia. PLoS One 11:e0163271. https://doi.org/10.1371/journal.pone.0163271.